



Application of the Avrami Theory for Wax Crystallisation of Synthetic Crude Oil

A. Hosseinipour^{*a}, A. Japper-Jaafar^b, S. Yusup^c, L. Ismail^d

^a Chemical Engineering Department, Universiti Teknologi PETRONAS, Perak Darul Ridzuan, Malaysia

^b Centre for Advanced and Professional Education, Universiti Teknologi PETRONAS, Kuala Lumpur, Malaysia

^c Biomass Processing Laboratory, Centre for Biofuel and Biochemical Research, Institute of Sustainable Living, Universiti Teknologi PETRONAS, Seri Iskandar, Perak, Malaysia

^d Faculty of Agro-Based Industry, Universiti Malaysia Kelantan, Kelantan, Malaysia

PAPER INFO

Paper history:

Received 13 July 2018

Received in revised form 16 December 2018

Accepted 03 January 2019

Keywords:

Paraffin

Wax Crystallisation

Differential Scanning Calorimetry

Avrami Theory

ABSTRACT

Wax crystallisation and deposition from offshore reservoirs have been causing serious problems such as plugged pipelines and reduced production flow rates. This issue is receiving more attention from the researchers and for commercial applications due to the shift in trend from using offshore production facilities to pipelines utilization. The aim of this study is the implementation of the Avrami theory to comprehend the mechanism of wax crystallisation to reveal the morphology of wax crystal using gravimetric and differential scanning calorimetry (DSC) analyses. The experiment values obtained from the Avrami's theory for both gravimetric and DSC techniques shows that the crystals were one-dimensional with rod-like structures.

doi: 10.5829/ije.2019.32.01a.03

NOMENCLATURE

ASTM	American society for testing and materials
GC	Gas Chromatography
FID	Flame Ionization Detector
X	Degree of crystallisation
K	Growth rate (min ⁻¹)
n	Avrami exponent
PP	Pour point
WAT	Wax appearance temperature

Greek Symbols

δ_{∞}	The maximum or asymptotic deposition (%)
δ_t	Relative deposition (%)
V_t	Volume or volume fraction of crystallisation
δ_t	The total deposition at time t (%)
δ_0	Initial wax in liquid (%)

1. INTRODUCTION

The relevancy of the paraffin deposition problem is now more pronounced and inevitable, owing to the fact that crude production has extended to offshore and ultra-deep oceans, with colder environments. However, the mitigation of paraffin deposition in the course of petroleum production has been an expensive process and has reduced the production activities in many oilfields around the globe. Production of crude oil from

offshore reservoirs has been facing severe difficulties such as plugged pipelines which deter the flow rate of production due to wax precipitations and depositions. This issue is gaining more attention due to the shift in the trend from offshore production facilities to pipelines utilization [1]. This shift satisfies both environmental and economic demands. Therefore, the importance of transporting waxy crude oils in surrounding seawater (277K in deep waters) has gained more attention in the oil industry [2-5].

Paraffin deposition and wax crystallisation depend on removal of wax deposits, predictions and prevention may cause blockage of the crude oil in the flowline. Numerous efforts which involve chemical treatments

*Corresponding Author Email: aryahpr@gmail.com (A. Hosseinipour)

have been utilized to rectify wax crystallisation issues such as the application of additional chemical inhibitors, mechanical means including regular pigging of pipelines, thermal treatment involving circulation of warm liquid, and a reliable thermodynamic model based on experimental data to determine wax equilibria [4, 6-16].

Wax structures or morphology is one of the factors which have attracted much interest to comprehend wax crystallisation or precipitation, deposition and gelation in production facilities and transportation pipelines [1, 10, 17, 18]. Over the past few decades, several studies in the field of wax deposition have highlighted the importance and applications of Avrami theory in the oil industry. These studies have implemented the non-gravimetric methods such as a cold finger, differential scanning calorimetry and rheometry [19-26] and gravimetric methods such as the oscillatory baffled tube apparatus [27]. The gravimetric experimental method was used according to Avrami theory to comprehend the mechanism and wax crystallisation kinetics. In the study by Lukman *et al.* [27] on the percentage of wax deposition, two opposite effects were observed by the oscillatory motion. Firstly, without the presence of any wax inhibitor or solvent at a low concentration of wax in the solution, oscillation considerably reduced the wax deposition by 40 to 60%. It also positively helped to prevent wax gelation from happening. Secondly, it had not been shown to prevent wax deposition; however, oscillatory motion accelerated the growth of the crystal to reach hundred percent wax deposition which was considered the disadvantage of this technique. However, less experimental attention has been devoted to the implementation of the gravimetric analysis to comprehend the kinetics and mechanism of wax crystallisation according to Avrami theory.

This study focused on wax crystallisation kinetics. The data acquisition required a shorter time to enable prediction, precipitation, and deposition for the oil inside the pipes and other facilities due to gravity. In addition, differential scanning calorimetry (DSC) was utilized to study Avrami theory on wax crystallisation mechanism and to reveal the morphology of wax crystal.

2. THE AVRAMI MECHANISM

In the oil pipelines, the wax crystallisation and deposition take place through the nucleation and crystallisation process. This process causes the oil to be trapped inside a network of crystals leading to gel formation, which can be termed as 'bulk crystallisation' [28]. In describing the crystallisation kinetics, the most reputable principle has been applied, i.e., Avrami phase transition equation, which describes how solids

transform from one phase (state of matter) to another specifically description of the kinetics of crystallisation [29]. The molecular diffusion mechanism is considered as one of the dominant wax deposition mechanisms which have been widely accepted and used.

The crystallisation process is expected to start randomly at various locations from the nucleation sites and spread outwards. This is demonstrated by the conception of raindrops dropping in a pool creating wave circles that cross over each other while expanding to the whole surface. The raindrops may fall all at once or sporadically. Similarly, they may hit the surface of the pool randomly at different points. The waves' expanding circles are viewed as the growth front of the spherulites, while the impact points are considered the crystallite nuclei [27]. Using probability derivations [30], the degree of crystallinity, X , which is considered the volume fraction of the crystalline material, could be shown as the following:

$$1 - X = e^{-E} \quad (1)$$

the average number of all fronts in the system is represented by E . A suitable approximation of $X \approx E$ can be considered for the low degree of crystallinity. E in the exponent of Equation (1) for the bulk crystallisation will be likely considered as the volume fraction or the volume of the crystalline materials, V_i , and therefore,

$$1 - X = e^{-V_i} \quad (2)$$

In bulk crystallisation, Equation (2) has been extensively recognized and applied to describe crystallisation [25, 31, 32]. This equation could be taken into account for sporadic or instantaneous nucleation and it could be shown as the following:

$$1 - X = e^{-Kt^n} \quad (3)$$

K denotes the growth rate (min^{-1}), and n is the so-called Avrami exponent representing the nucleation's nature and characterizes the crystal structure, and t is time (s) [33].

The present study uses the relative wax deposition to measure the degree of crystallinity (δ_r) being the deposition's mass fractions on the test tube wall divided by the initial mass of the wax-oil liquid:

$$\delta_r = (\delta_t - \delta_0) / (\delta_\infty - \delta_0) \quad (4)$$

Where δ_t represents the total deposition at time t (min), wt%, δ_0 the initial mass of the wax content in the liquid, (g) and δ_∞ the asymptotic or maximum deposition attained from the deposition curves when the quasi-steady state or the asymptotic condition has been accomplished (g). Replacing X by δ_r from Equation (4) and taking log twice in Equation (3), it can be written as follows:

$$\log(-\ln(1-\delta_r)) = \log K + n \log(t) \quad (5)$$

As a result of plotting the $\log(t)$ versus the left side in Equation (5), the intersection K and the slope of the straight line n can be found. The Avrami coefficient is helpful in understanding the mechanism of phase transformation and its effect on both nucleation and growth. Hay [34] derived a model for rods, discs and spheres using both K and n as the indicative tool of crystallisation mechanism to represent one-, two- and three-dimensional forms of growth, which are summarized in Table 1. The Avrami exponent (n) has been frequently utilized in order to draw a distinction between different crystallisation mechanisms [35]; moreover, its theoretical value (1, 2, 3, or 4, etc.) is defined by the crystal growth and nucleation's nature. Rod-like crystals represented by $n=1$ correspond to the growth of instantaneous nuclei; while, $n=3$ or 4 indicates spherulitic growth from either instantaneous or sporadic nucleation [36].

3. EXPERIMENTAL WORK

3.1. Materials Paraffin wax was purchased from Merck kGaA, Darmstadt, Germany, and it was in pastille form with a solidification point of 324-326K. Diesel fuel was purchased from a PETRONAS petrol station in Malaysia and was used as the solvent.

3.2. Experimental Apparatus and Method In this work, a cooling thermostat (Lauda Alpha RA24) from LAUDA-Brinkmann, LP was used to control the test temperature. Also, a magnetic hotplate stirrer (Lab-Mix 20) from Fisher Scientific was used for heating and stirring the sample.

TABLE 1. The Avrami parameters for crystallisation of polymers [34]

Crystallisation mechanism	n	Growth form
Spheres		
Sporadic	4	Three dimensions
Instantaneous	3	Three dimensions
Discs ^a		
Sporadic	3	Two dimensions
Instantaneous	2	Two dimensions
Rods ^b		
Sporadic	2	One dimension
Instantaneous	1	One dimension

^a Constant thickness.

^b Constant radius.

A synthetic crude oil was made by adding 10% of the paraffin wax weight into diesel placed on a magnetic hotplate stirrer at a temperature of 323.15K to obtain a homogeneous solution. The wax concentration was fixed for all the experiments at 10% weight. Prior to any experiments, the synthetic crude oil was thoroughly covered to prevent evaporation then heated to a temperature of 323.15K using a magnetic hotplate stirrer at a speed of 200 rpm to dissolve the solid wax. The same procedure was repeated for all the experiments.

The GC Clarus 580 from PerkinElmer and a capillary column for Agilent J&W DB-2887 column were utilized to detect the normal alkynes and their compositions. This column is specifically designed for simulated distillation of ASTM Method D2887. Gas Chromatography-Flame Ionization Detector (GC-FID) was utilized by the Clarus 580 GC equipped with a 100% Dimethylpolysiloxane capillary column (10m × 0.530 mm × 3 μm) with part number 125.2814, and Nitrogen as the carrier gas. The CS₂ was used as a solvent to dissolve samples before injection. The samples were prepared at a concentration of about 25 mass percent in the solvent (CS₂). An injection containing one μL of the solution was prepared followed by heating in the oven for 2 minutes of equilibration at 298.15K and from 313.15K to 623.15K at a rate of 10K/min, and subsequently, the temperature was held constant for 31 min at the final temperature.

3.3. Nucleation and Crystallisation Analysis using the Gravimetric Method based on Avrami Equation

According to the ASTM D2500 and ASTM D97, 40ml is the best volume for evaluating the cloud point and pour point. The initial temperature T_1 was adjusted at 323.15K, considering it was well above the wax appearance temperature (WAT) of the synthetic crude oil to allow complete dissolution. Various temperatures lower than the WAT were selected for T_2 (278.15, 283.15, 288.15 and 293.15K). T_2 refers to the wall temperature which is controlled by cooling a thermostat. The cloud point and pour point of the sample were measured according to the ASTM D2500 and ASTM D97, respectively. The cloud point was measured 301.15K by observing the onset of cloudiness of the solution and the pour point was measured to be 297.15K by observing the lowest temperature at which the specimen did not show any movement when tilted.

As depicted in Figure 1, a schematic graph of the wax deposition system is similar to the pipe in reality during shut-in procedures. The system involves a cold bath with water circulation which helps to maintain the temperature of the water and a test tube to examine the deposition of wax.

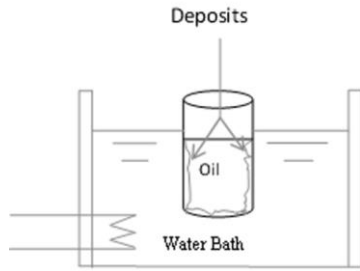


Figure 1. A sketch of the wax deposition system

After the synthetic crude oil was heated using a magnetic hotplate stirrer to dissolve the solid wax, a 40ml volume was evaluated by using a measuring cylinder before being pouring into a test tube. A 10-minute time was considered as the typical experimental duration to measure wax deposition. The measurements were made at time intervals of 1, 2, 3, 5, 7 and 10 minutes.

The amount of mass deposition was measured using the gravimetric method. Initially, the synthetic crude oil was heated up to T_i (323.15K) for about 20 minutes while stirring to allow all of the paraffin waxes to dissolve into the liquid. The desired volume was obtained using the measuring cylinder and was then transferred to the test tube. The mass of each volume was measured based on an analytical lab scale and then the sample was immersed into the cooling thermostat so that an axially symmetric thermal field was produced through the sample. After each desired time, the test tube was taken out, the non-deposited part of the sample was drained out through gravity to a beaker and then the deposited wax was weighted. The same procedure was repeated for different volumes and temperatures. At the end, the amount of deposit was measured as a weight percentage of the total wax. To confirm repeatability, the experiments were measured in triplicate.

3. 4. Nucleation and Crystallisation Analysis using the DSC Method based on Avrami Equation

Chen et al. [37] found a good linear relation between the Q_{oil} and the related wax contents defined individually by Q_{oil}/Q_{wax} and standard acetone methods. There is a linear relationship between the corresponding wax contents and the Q_{oil} represented via Equation (6) with a R-squared of 0.9837.

$$C_{wax} = 0.75Q_{oil} + 0.2 \quad (6)$$

where the total thermal effect Q of crude oil between the WAT and 253.15K (-20°C) is Q_{oil} (J/g), and C_{wax} (wt.%) is the wax content. The linear relation between the wax contents calculated by the standard acetone method and the Q_{oil} is shown in Equation (7) with an R-squared 0.9651.

$$C_{wax} = 0.73Q_{oil} + 0.74 \quad (7)$$

Based on the empirical correlations in Equations (6) and (7) and assuming that the Q_{oil} (J/g) was calculated in the temperature range from the WAT to 253.15K (-20°C), the wax content of the synthetic crude oil was calculated as $C_{wax} = 10.34$ and $C_{wax} = 10.64$ for the DSC and the acetone standard method, respectively. The wax content values were slightly above the 10 percent by weight when paraffin wax was added to diesel to produce synthetic crude oil. However, Q_{oil} of the synthetic crude oil was not calculated based on Chen *et al.* [37]'s method (i.e. the sample was not run from the WAT to 253.15K (-20°C)). Therefore, corrections and adjustments (extrapolation to 253.15K (-20°C)) were then necessary to calculate the percentage of the total wax content precipitated from WAT to approximately 283.15K (10°C).

Figures 2 and 3 show the total heat release for the pure paraffin wax with the synthetic crude oil being -157.284 (J/g) and -13.521 (J/g), respectively. In Figure 2, it is assumed that the crystallisation process is complete when the starting point (WAT) and the ending point of the baseline meet each other. According to Chen *et al.* [37]'s method, it can be seen from Figure 3 that the crystallisation process has not been completed.

Based on Chen *et al.* [37], the wax content calculated by Q_{oil}/Q_{wax} showed that the analysis and calculation of the pure paraffin wax has 100% wax content by weight (Figure 2). However, due to incomplete crystallisation in the synthetic crude oil, the Q_{oil}/Q_{wax} is about 8.6% which is 86% of the total wax crystallisation. The total crystallisation heat of the synthetic crude oil contributed to the total 86% (-13.521 J/g) of the heat released from the WAT to 283.15K (10°C) plus the remaining 14% (-1.893J/g) from 283.15K (10°C) to 253.15K (-20°C). As the total crystallisation heat became -15.414 (J/g), Chen *et al.* [37]'s correlation for the DSC technique (Equation 6) could be rewritten as follows:

$$C_{wax} = 0.635|Q_{oil}| + 0.2 \quad (8)$$

which can be considered under the condition that the sample can run only until 283.15K (10°C). All the calculations in the Avrami's theory by DSC are based on this new correlation (Equation (8)).

From the DSC curves in determination of the wax solubility curve done by Alcazar-Vara and Buenrostro-Gonzalez [38], the values of the relative crystallinity $X(T)$ at various cooling rates can be measured. The relative crystallinity can be written as a function of temperature as below:

$$X(T) = \frac{\int_{T_0}^T (dH_c / dT) dT}{\Delta H_c} \quad (9)$$

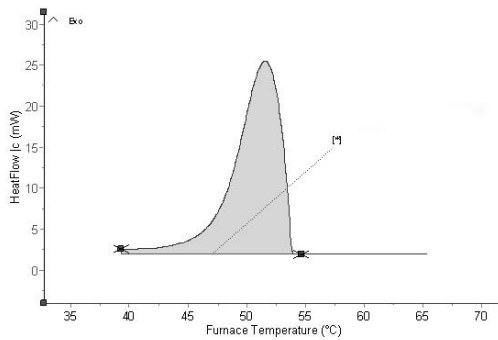


Figure 2. The DSC thermograph of the pure paraffin wax

*[Heat: -157.284 (J/g)
 T: 54.68 and 39.30 (°C)
 Peak Maximum: 51.563 (°C) / 1,296 (s)
 Peak Height: 23.631 (mW)
 Onset: 53.826 (°C) / 1,168.08 (s)
 Offset: 47.329 (°C) / 1,558.26 (s)
 Baseline Type: Tangential First Point]

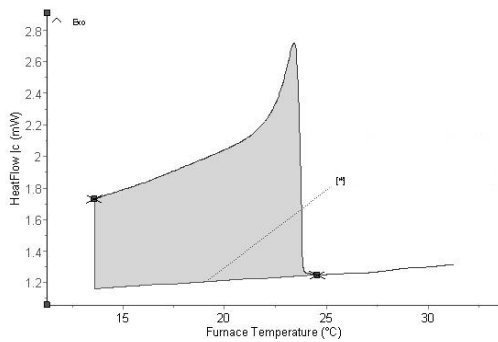


Figure 3. The DSC thermograph of the synthetic crude oil

*[Heat: -13.521 (J/g)
 T: 24.57 and 13.61 (°C)
 T: 1,134.6 and 1,800.0 (s)
 Peak Maximum: 23.382 (°C) / 1,205.2 (s)
 Peak Height: 1.187 (mW)
 Onset: 23.823 (°C) / 1,186.774 (s)
 Offset: 20.758 (°C) / 1,378.739 (s)
 Baseline Type: Tangential First Point]

where dH_c is the crystallization's enthalpy released in an infinitesimal temperature range dT , T_0 and T related to the onset and arbitrary temperatures, correspondingly. And for a specific cooling range, ΔH_c is the total enthalpy of crystallization.

Based on the procedure which was explained above, Avrami method is used to analyze the crystallisation kinetics and the equation can be written as:

$$1 - X(t) = \exp(-Kt^n) \quad (10)$$

or

$$\log(-\ln[1 - X(t)]) = \log K + n \log t \quad (11)$$

4. RESULTS AND DISCUSSIONS

In this research, the gravimetric method [27] is used to study the effect of different volumes and temperatures on nucleation and crystallisation of synthetic crude oil. This section discusses the Avrami theory using firstly the gravimetric and secondly the DSC techniques to investigate the wax crystallisation kinetics of the synthetic crude oil.

4. 1. Characterization of the Synthetic Crude Oil and Paraffin Wax

The paraffin wax and synthetic crude oil's compositions are characterized by GC-FID based on the ASTM-D2887. The analyses are presented in Tables 2 and 3. The crystallisation point, physical form and their structures are based on a handbook of chemistry and physics and a handbook of data on common organic compounds [39-41]. One of the reasons for wax crystallisation issue lies in the molecular composition of the wax molecules and their interactions in the crude oil. These interactions are caused by VdW forces which have a direct influence on wax crystallisation [42].

The results based on the crystallisation point, physical form, types of hydrocarbons and their structures show that this synthetic crude oil consists of normal paraffins, and thus have a tendency towards wax crystallisation and deposition in transportation pipelines. Table 3 shows that this tendency might be higher for this synthetic crude oil due its content of normal paraffins with carbon atom numbers greater than 16 [43]. Therefore, as a general practice, utilization of a wax inhibitor, regular pigging, thermal treatment and other remediation strategies are necessary to avoid pipeline plugging.

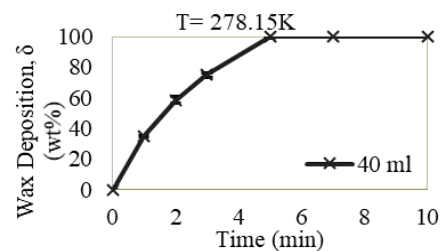
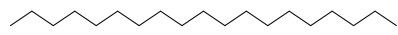
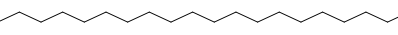
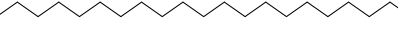



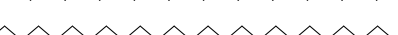

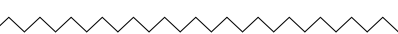
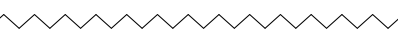
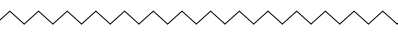
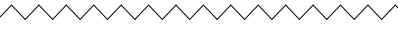
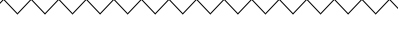






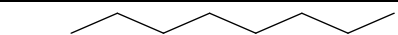
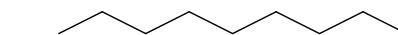
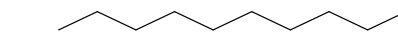
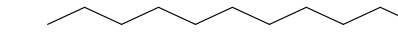
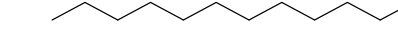
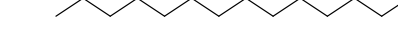
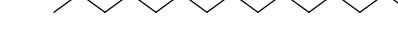

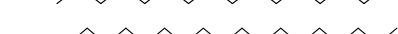

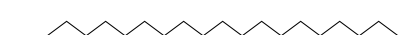
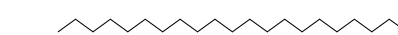

Figure 4. The effect of different volumes on wax deposition at a constant temperature

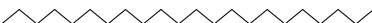












TABLE 2. Analysis of the paraffin wax

Components	Formula	Crystal- isaion Point (K)	Physical form	H/C type	Raw Amount	Relative Compositio n ^a (wt %)	Structure
Nonadecane	C ₁₉ H ₄₀	305.15	solid	N-P	0.0005	0.0997	
Eicosane	C ₂₀ H ₄₂	309.75	solid	N-P	0.0026	0.5315	
Heneicosane	C ₂₁ H ₄₄	313.65	solid	N-P	0.0125	2.5136	
Docosane	C ₂₂ H ₄₆	317.55	solid	N-P	0.0391	7.8286	
Tricosane	C ₂₃ H ₄₆	320.91	solid	N-P	0.0780	15.5907	
Tetracosane	C ₂₄ H ₅₀	323.55	solid	N-P	0.1107	22.1349	
Pentacosane	C ₂₅ H ₅₂	327.08	solid	N-P	0.1047	20.9279	
Hexacosane	C ₂₆ H ₅₄	329.25	solid	N-P	0.0768	15.3693	
Heptacosane	C ₂₇ H ₅₆	332.65	solid	N-P	0.0418	8.3490	
Octacosane	C ₂₈ H ₅₈	337.65	solid	N-P	0.0178	3.5544	
Nonacosane	C ₂₉ H ₆₀	336.85	solid	N-P	0.0066	1.3177	
Triacontane	C ₃₀ H ₆₂	338.25	solid	N-P	0.0028	0.5536	
Hentriacontane	C ₃₁ H ₆₄	341.05	solid	N-P	0.0016	0.3211	
Dotriacontane	C ₃₂ H ₆₆	342.85	solid	N-P	0.0024	0.4761	
Tritriacontane	C ₃₃ H ₆₈	344.35	solid	N-P	0.0002	0.0332	
Hexatriacontane	C ₃₆ H ₇₄	348.95	solid	N-P	0.0014	0.2879	
Tetracontane	C ₄₀ H ₈₂	354.65	solid	N-P	0.0006	0.1107	
Unknown			0.16 ^b		0.0009 ^c		
Unknown			0.05 ^b		0.0003 ^c		

a: $Relative\ Composition\ (wt\ \%) = \frac{Peak\ area\ of\ desired\ componet}{Peak\ area\ of\ n - alkanes\ (C_{19} - C_{40})} \times 100$ b; c: Peak area %; Raw amount

TABLE 3. Analysis of the synthetic crude oil

Components	Formul a	Crystal- isaion Point (K)	Physical form	H/C type	Raw amount	Relative Composition ^a (wt %)	Structure
Octane	C ₈ H ₁₈	216.33	solid	N-P	0.0068	0.3235	
Nonane	C ₉ H ₂₀	219.69	solid	N-P	0.0059	0.2894	
Decane	C ₁₀ H ₂₂	243.55	solid	N-P	0.0353	1.7024	
Undecane	C ₁₁ H ₂₄	247.65	solid	N-P	0.0695	3.3538	
Dodecane	C ₁₂ H ₂₆	263.58	solid	N-P	0.0586	2.8260	
Tetradecane	C ₁₄ H ₃₀	278.97	solid	N-P	0.1756	8.4610	
Pentadecane	C ₁₅ H ₃₂	283.1	solid	N-P	0.2170	10.4528	
Hexadecane	C ₁₆ H ₃₄	291.27	solid	N-P	0.2158	10.4018	
Heptadecane	C ₁₇ H ₃₆	295.15	solid	N-P	0.1913	9.2271	
Octadecane	C ₁₈ H ₄₀	301.35	solid	N-P	0.1921	9.2612	
Nonadecane	C ₁₉ H ₄₀	305.15	solid	N-P	0.1927	9.2952	
Eicosane	C ₂₀ H ₄₂	309.75	solid	N-P	0.1058	5.1073	
Heneicosane	C ₂₁ H ₄₄	313.65	solid	N-P	0.1431	6.8948	

Docosane	C ₂₂ H ₄₆	317.55	solid	N-P	0.1142	5.5158	
Tricosane	C ₂₃ H ₄₆	320.91	solid	N-P	0.0846	4.0688	
Tetracosane	C ₂₄ H ₅₀	323.55	solid	N-P	0.0968	4.6646	
Pentacosane	C ₂₅ H ₅₂	327.08	solid	N-P	0.0769	3.7113	
Hexacosane	C ₂₆ H ₅₄	329.55	solid	N-P	0.0485	2.3323	
Heptacosane	C ₂₇ H ₅₆	332.65	solid	N-P	0.0234	1.1236	
Octacosane	C ₂₈ H ₅₈	337.65	solid	N-P	0.0102	0.4937	
Nonacosane	C ₂₉ H ₆₀	336.85	solid	N-P	0.0049	0.2383	
Triacontane	C ₃₀ H ₆₂	338.25	solid	N-P	0.0022	0.1021	
Dotriacontane	C ₃₂ H ₆₆	342.85	solid	N-P	0.0013	0.0681	
Tritriacontane	C ₃₃ H ₆₈	344.35	solid	N-P	0.0002	0.0170	
Hexatriacontane	C ₃₆ H ₇₄	348.95	solid	N-P	0.0011	0.0511	
Tetratetracontane	C ₄₄ H ₉₀	358.75	solid	N-P	0.0004	0.0170	
Unknown					3.47 ^b	0.1227 ^c	
Unknown					2.71 ^b	0.0959 ^c	
Unknown					0.06 ^b	0.0019 ^c	
Unknown					0.06 ^b	0.0022 ^c	

a:
$$\text{Relative Composition (wt \%)} = \frac{\text{Peak area of desired component}}{\text{Peak area of } n\text{-alkanes (C}_{19}\text{ - C}_{40})} \times 100$$

b, c: Peak area %; Raw amount

4. 1. The Mechanism of Crystallisation Based on the Avrami Theory Using the Gravimetric Technique

From the deposition profile demonstrated in Figure 4, the formation of wax can be generally categorized into three main divisions: the nucleation phase, the growth phase and the quasi-steady state. The first and second sections are combined as a single step as the nucleation is too fast to be measured in most related studies [27]. Usually, the growth phase occurred in the first 2 or 3 minutes of the experiments for most of the solutions. Using the Avrami theory to analyze the growth phase curves, one can extract some crystallisation/deposition kinetics.

Figure 5 plots $\log(-\ln(1-\delta_r))$ versus $\log(t)$ to obtain the Avrami parameters using the gravimetric technique. Good linearity is seen in this figure for the gravimetric techniques which demonstrates the efficiency of the Avrami theory. The temperature difference is defined as the pour point minus the test temperature (T_2). It was observed that for the 40ml volume the temperature difference decreased, where the Avrami's exponent values were found to be between 1 to 1.44 indicating that the crystals were one-dimensional and rod-like. An Olympus BX53 cross-polarized optical microscope instrument was used to obtain the crystal shape in Figure 6. Clearly the shapes of crystals shown in Figure 6 are matched well with kinetic evaluations. With an increase in the Avrami's exponent, the

crystallization mechanism changed from instantaneous to sporadic. This is observed for testing temperatures closer to the pour point, i.e. smaller temperature differences.

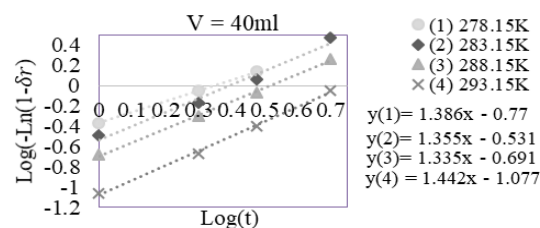


Figure 5. The effect of different temperatures on the Avrami parameters at a constant volume of 40ml

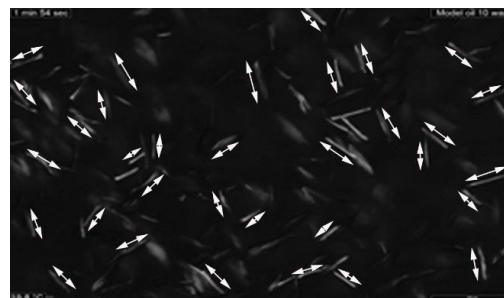


Figure 6. The wax structure of the synthetic crude oil at 293.15K

Lukman et al. [27] employed an oscillatory baffled tube device in order to develop an understanding of the mechanism and wax crystallisation kinetics through the gravimetric experimental technique according to the Avrami theory. He concluded that without the oscillation, the wax crystals were in one-dimensional growth and of a rod-like shape. However, at 10% wax concentration due to oscillatory motion, the Avrami constants approached four indicating the change from needle-like crystals into sphere-like crystals. This observation was verified by a microscope showing the crystals' shape that clearly matched well with the kinetic analyses.

4. 2. The Mechanism of Crystallisation Based on the Avrami Theory Using the DSC Technique

The measurement norm of DSC relies on the examination of the variance in the heat flows to the sample cell and the reference cell. These heat flows are linearly proportional to the temperature variance between the cell and the furnace. However, it is inversely proportional to the thermal resistance of the system mentioned above. This method is based on the detection of heat released during crystallization, which gives rise to an exothermic peak on cooling [44].

In Equation (12), through plotting the left side versus $\log(t)$, the intersection K and the slope of the straight line n can be found, where K denotes the growth rate and n is the so-called Avrami exponent which represents the nucleation's nature and characterizes the structure of the crystal, and t is time.

The result of the Avrami kinetics analyses in Figure 7 point out that the Avrami's exponent value is 1.5418. Based on the Avrami's exponent value, the crystals would be of a rod-like shape in one-dimensional growth. Obviously, the shapes of the crystals presented in Figure 6 are corresponding well with the kinetic analyses. On this account, the Avrami kinetics analyses could be considered as a reliable method to comprehend the kinetics and mechanism of the wax crystallisation by using the DSC technique.

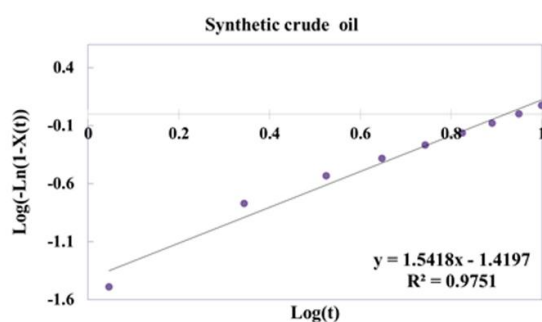


Figure 7. Plot of $\log(-\ln(1-X(t)))$ vs. $\log(t)$ to obtain the Avrami parameters using the DSC technique

5. CONCLUSIONS

The Avrami theory was successful in determination of the initiation of wax crystallisation. Based on the Avrami exponent values (n) (1 to 1.44 and 1.54) for the gravimetric and DSC technique respectively, the crystals were one-dimensional, rode-like or needle-like. Both gravimetric and differential scanning calorimetry techniques were successful in defining the crystallisation kinetics and the shape of crystals.

6. ACKNOWLEDGMENT

The authors wish to thank Universiti Teknologi PETRONAS (UTP), for providing financial support in this study. The authors also would like to express their appreciation to Dr. Bhajan Lal and Dr. Behzad Partoon from phase separation lab for his assistance in providing the lab facilities.

7. REFERENCES

1. Kjøråas, M., "Structure of paraffin wax deposits in subsea pipelines", Norwegian University of Science and Technology, Department of Petroleum Engineering and Applied Geophysics, (2013).
2. Singh, A., Lee, H.S., Singh, P. and Sarica, C., "Flow assurance: Validation of wax deposition models using field data from a subsea pipeline", in Offshore Technology Conference, Offshore Technology Conference, (2011).
3. Lee, H.S., "Computational and rheological study of wax deposition and gelation in subsea pipelines, ProQuest, (2008).
4. Huang, Z., Lee, H.S., Senra, M. and Scott Fogler, H., "A fundamental model of wax deposition in subsea oil pipelines", *AIChE Journal* Vol. 57, No. 11, (2011), 2955-2964.
5. Ribeiro, F.S., Souza Mendes, P.R. and Braga, S.L., "Obstruction of pipelines due to paraffin deposition during the flow of crude oils", *International Journal of Heat and Mass Transfer* Vol. 40, No. 18, (1997), 4319-4328.
6. Creek, J., Lund, H.J., Brill, J.P. and Volk, M., "Wax deposition in single phase flow", *Fluid Phase Equilibria* Vol. 158, No., (1999), 801-811.
7. Nasrifar, K. and Moshfeghian, M., "Multiphase equilibria of waxy systems with predictive equations of state and a solid solution model", *Fluid Phase Equilibria* Vol. 314, No., (2012), 60-68.
8. Wu, Y., Ni, G., Yang, F., Li, C. and Dong, G., "Modified maleic anhydride co-polymers as pour-point depressants and their effects on waxy crude oil rheology", *Energy & Fuels*, Vol. 26, No. 2, (2012), 995-1001.
9. Alcazar-Vara, L.A. and Buenrostro-Gonzalez, E., Liquid-solid phase equilibria of paraffinic systems by dsc measurements. N: Elkordy, a.A. (ed.), applications of calorimetry in a wide context—differential scanning calorimetry, iso-thermal titration calorimetry and microcalorimetry, intech, rijeka, croatia, pp. 253–276. 2013.
10. Jafari Ansaroudi, H., Vafaie-Sefti, M., Masoudi, S., Behbahani, T.J. and Jafari, H., "Study of the morphology of wax crystals in the presence of ethylene-co-vinyl acetate copolymer",

- Petroleum Science and Technology* Vol. 31, No. 6, (2013), 643-651.
11. Chala, G.T., Sulaiman, S.A., Japper-Jaafar, A., Abdullah, W.A.K.W. and Mokhtar, M.M.M., "Gas void formation in statically cooled waxy crude oil", *International Journal of Thermal Sciences*, Vol. 86, No., (2014), 41-47.
 12. Kok, M., "The effect of pour point depressant on the flow behavior of crude oils", *Energy Sources, Part A: Recovery, Utilization, and Environmental Effects*, Vol. 36, No. 2, (2014), 167-172.
 13. Zhang, F., Ouyang, J., Feng, X., Zhang, H. and Xu, L., "Paraffin deposition mechanism and paraffin inhibition technology for high-carbon paraffin crude oil from the kazakhstan pk oilfield", *Petroleum Science and Technology* Vol. 32, No. 4, (2014), 488-496.
 14. Zhang, H., "Study on paraffin removal additive of high wax crude oil", in *Advanced Materials Research*, Trans Tech Publications Vol. 960, No. Issue, (2014), 11-13.
 15. Quan, Q., Gong, J., Wang, W. and Wang, P., "The influence of operating temperatures on wax deposition during cold flow and hot flow of crude oil", *Petroleum Science and Technology* Vol. 33, No. 3, (2015), 272-277.
 16. Vafaie-Sefti, M., Mousavi-Dehghani, S. and Bahar, M.M.-Z., "Compositional modeling of wax formation in petroleum mixtures", *International Journal of Engineering, Transactions A: Basics*, Vol. 14, No. 4, (2001), 303-312.
 17. Kané, M., Djabourov, M., Volle, J.-L., Lechaire, J.-P. and Frebourg, G., "Morphology of paraffin crystals in waxy crude oils cooled in quiescent conditions and under flow", *Fuel*, Vol. 82, No. 2, (2003), 127-135.
 18. Askari, S., "Oil reservoirs classification using fuzzy clustering", *International Journal of Engineering, Transactions C: Aspects*, Vol. 30, No. 9, (2017), 1391-1400.
 19. Hammami, A. and Mehrotra, A.K., "Non-isothermal crystallization kinetics of n-paraffins with chain lengths between thirty and fifty", *Thermochimica Acta*, Vol. 211, No. 0, (1992), 137-153.
 20. Svetlichnyy, D., Didukh, A., Aldyarov, A., Kim, D., Nawrocki, M. and Baktygali, A., "Study of heat treatment and cooling rate of oil mixtures transported by "kumkol-karakoin-barsengir-atasu" pipeline", *Electronic Scientific Journal "Oil and Gas Business*, Vol., No. 2, (2011), 427-437.
 21. Ekweribe, C.K., Civan, F., Lee, H.S. and Singh, P., "Interim report on pressure effect on waxy-crude pipeline-restart conditions investigated by a model system", *SPE Projects Facilities & Construction*, Vol. 4, No. 03, (2009), 61-74.
 22. Zougari, M.I. and Sopkow, T., "Introduction to crude oil wax crystallization kinetics: Process modeling", *Industrial & Engineering Chemistry Research*, Vol. 46, No. 4, (2007), 1360-1368.
 23. Primicerio, M., Wax segregation in oils: A multiscale problem, in *Progress in industrial mathematics at ecmi 2008*. 2010, Springer.43-67.
 24. Lopes-da-Silva, J. and Coutinho, J.A., "Analysis of the isothermal structure development in waxy crude oils under quiescent conditions", *Energy & Fuels*, Vol. 21, No. 6, (2007), 3612-3617.
 25. Pal, S. and Nandi, A.K., "Cocrystallization mechanism of poly (3-alkyl thiophenes) with different alkyl chain length", *Polymer*, Vol. 46, No. 19, (2005), 8321-8330.
 26. Caze, C., Devaux, E., Crespy, A. and Cavrot, J., "A new method to determine the avrami exponent by dsc studies of non-isothermal crystallization from the molten state", *Polymer*, Vol. 38, No. 3, (1997), 497-502.
 27. Ismail, L., Westacott, R.E. and Ni, X., "On the effect of wax content on paraffin wax deposition in a batch oscillatory baffled tube apparatus", *Chemical Engineering Journal* Vol. 137, No. 2, (2008), 205-213.
 28. Singh, P., Venkatesan, R., Fogler, H.S. and Nagarajan, N., "Formation and aging of incipient thin film wax-oil gels", *AIChE Journal* Vol. 46, No. 5, (2000), 1059-1074.
 29. Avrami, M., "Kinetics of phase change. I general theory", *The Journal of Chemical Physics*, Vol. 7, No. 12, (1939), 1103-1112.
 30. Sperling, L.H., "Kinetics of crystallisations, in: L.H. Sperling (ed.), introduction to physical polymer science", *John Wiley and Sons*, (1986), 271-291.
 31. Cazé, C., Devaux, E., Crespy, A. and Cavrot, J.P., "A new method to determine the avrami exponent by d.S.C. Studies of non-isothermal crystallization from the molten state", *Polymer*, Vol. 38, No. 3, (1997), 497-502.
 32. Lu, M., Shim, M. and Kim, S., "Curing behavior of an unsaturated polyester system analyzed by avrami equation", *Thermochimica Acta*, Vol. 323, No. 1, (1998), 37-42.
 33. Avrami, M., "Kinetics of phase change. Ii transformation-time relations for random distribution of nuclei", *The Journal of Chemical Physics*, Vol. 8, No. 2, (1940), 212-224.
 34. Hay, J., "Application of the modified avrami equations to polymer crystallisation kinetics", *Polymer International* Vol. 3, No. 2, (1971), 74-82.
 35. Campos, R., Litwinenko, J. and Marangoni, A., "Fractionation of milk fat by short-path distillation", *Journal of Dairy Science* Vol. 86, No. 3, (2003), 735-745.
 36. Sharples, A., "Overall kinetics of crystallisation, in: A. Sharples (ed.), introduction to polymer crystallisation", *Edward Arnold Ltd., London*, Vol., No., (1966), 44-59.
 37. Chen, J., Zhang, J. and Li, H., "Determining the wax content of crude oils by using differential scanning calorimetry", *Thermochimica Acta*, Vol. 410, No. 1, (2004), 23-26.
 38. Alcazar-Vara, L.A. and Buenrostro-Gonzalez, E., "Experimental study of the influence of solvent and asphaltenes on liquid-solid phase behavior of paraffinic model systems by using dsc and fir techniques", *Journal of Thermal Analysis and Calorimetry* Vol. 107, No. 3, (2012), 1321-1329.
 39. Lide, D.R. and Milne, G.W., "Handbook of data on common organic compounds, CRC press, Vol. 3, (1995).
 40. Weast, R.C., Astle, M.J. and Beyer, W.H., "Crc handbook of chemistry and physics, CRC press Boca Raton, FL, Vol. 69, (1988).
 41. Weast, R.C. and Grasselli, J.G., "Handbook of data on organic compounds", Vol., No., (1989).
 42. Pauling, L., "General chemistry, Courier Corporation, (1988).
 43. Hosseinipour, A., Sabil, K.M., Arya Ekaputra, A., Japper, A.B. and Ismail, L.B., "The impact of the composition of the crude oils on the wax crystallization", in *Applied Mechanics and Materials*, Trans Tech Publications. Vol. 625, No. Issue, (2014), 196-200.
 44. Roenningsen, H.P., Bjoerndal, B., Baltzer Hansen, A. and Batsberg Pedersen, W., "Wax precipitation from north sea crude oils: I. Crystallization and dissolution temperatures, and newtonian and non-newtonian flow properties", *Energy & Fuels*, Vol. 5, No. 6, (1991), 895-908.

Application of the Avrami Theory for Wax Crystallisation of Synthetic Crude Oil

A. Hosseinipour^a, A. Japper-Jaafar^b, S. Yusup^c, L. Ismail^d

^a Chemical Engineering Department, Universiti Teknologi PETRONAS, Perak Darul Ridzuan, Malaysia

^b Centre for Advanced and Professional Education, Universiti Teknologi PETRONAS, Kuala Lumpur, Malaysia

^c Biomass Processing Laboratory, Centre for Biofuel and Biochemical Research, Institute of Sustainable Living, Universiti Teknologi PETRONAS, Seri Iskandar, Perak, Malaysia

^d Faculty of Agro-Based Industry, Universiti Malaysia Kelantan, Kelantan, Malaysia

PAPER INFO

چکیده

Paper history:

Received 13 July 2018

Received in revised form 16 December 2018

Accepted 03 January 2019

Keywords:

Paraffin

Wax Crystallisation

Differential Scanning Calorimetry

Avrami Theory

کریستالیزاسیون موم و رسوب از مخازن دریایی باعث مشکلات جدی مانند انسداد خطوط لوله و کاهش جریان تولید شده است. این موضوع از توجه محققان و برنامه های تجاری به دلیل تغییر روند استفاده از امکانات تولید دریایی به استفاده از خطوط لوله، بیشتر است. هدف از این مطالعه پیاده سازی تئوری آرومی برای درک مکانیسم بلورینگی موم است تا مورفولوژی کریستال موم را با استفاده از تجزیه و تحلیل اسکن کالری سنجی (DSC) و جاذبه سنجی نشان دهد. مقادیر آزمایشی حاصل از نظریه آرومی برای هر دو تکنیک جاذبه سنجی و DSC نشان می دهد که کریستال ها یک بعدی با ساختارهای میله ای مانند می باشند.

doi: 10.5829/ije.2019.32.01a.03
